Polymorphism

DOI: 10.1002/ange.200500081

Synthesis of Stable Aragonite Superstructures by a Biomimetic Crystallization Pathway**

Nadine Nassif, Nicole Gehrke, Nicola Pinna, Natasha Shirshova, Klaus Tauer, Markus Antonietti, and Helmut Cölfen**

Many organisms make use of calcium carbonate as a construction material, and for this purpose are able to selectively control the formation of the different polymorphs of this material. This is not the case for technical processes. Calcite is thermodynamically more stable at ambient pressure and temperature[1] than the other anhydrous $CaCO_3$ polymorphs (vaterite and aragonite), and thus is most easily obtained with long reaction times. There are some technical procedures which generate vaterite (usually the first polymorph formed as a result of the Ostwald rule of stages) by performing the precipitation along the kinetic pathway and yielding the kinetic metastable vaterite product or by trapping and stabilizing the very early crystals[2] with appropriate stabilizers. However, the mechanically very interesting aragonite (usually a high-pressure modification) is virtually inaccessible by chemical means, except by adding extreme amounts of Mg^{2+} ions to the mother liquor.[3,4] It should be recalled that nacre, with its extraordinary mechanical performance, is based on pure aragonite platelets[5] and shows clear long-time stability even in the presence of water. In contrast, aragonite usually starts to transform to calcite within a day or faster depending on the pH value and temperature.[6,7] Thus, one of the main challenges in the crystallization of calcium carbonate remains the synthesis of pure aragonite of uniform size and morphology under ambient conditions.

It has previously been described that aragonite is formed in a biomimetic pathway in the presence of several extracted

[*] Dr. N. Nassif, N. Gehrke, Dr. N. Shirshova, Dr. K. Tauer, Dr. M. Antonietti, Dr. H. Cölfen
Max-Planck Institute of Colloids and Interfaces
Colloid Chemistry
Research Campus Golm, 14424 Potsdam (Germany)
Fax: (+49) 331-567-9502
E-mail: nadine.nassif@mpikg-golm.mpg.de
coelfen@mpikg-golm.mpg.de

Dr. N. Pinna
Martin-Luther-Universität Halle-Wittenberg
Institut für Anorganische Chemie
Kurt-Mothes-Strasse 2, 06120 Halle (Saale) (Germany)

[**] We thank Dr. Cornelia Sinn, Dr. Reinhard Sigel, and Dr. Miles Page for their kind scientific assistance and the Deutsche Forschungsgemeinschaft for financial support within the priority program 1117: "Principles of Biomineralization". We also thank the Fritz Haber Institute and Prof. R. Schlögl for use of the electron microscope and Klaus Weiss for his technical assistance.

Supporting information for this article is available on the WWW under http://www.angewandte.org or from the author.

macromolecules from different shells in the presence[8] or absence[9] of an organic matrix, under compressed monolayers[10,11] or at the liquid–liquid interface in a radial Hele–Shaw cell.[12] More recently, aragonite was obtained as a metastable intermediate at the air–water interface by the use of a basic polymer.[13] Other reported ways to obtain aragonite include, for example, the transformation of amorphous calcium carbonate nanoparticles in reverse surfactant microemulsions,[14] by heat-induced precipitation onto self-assembled monolayers of anthracene-terminated thiol chains,[15] or by high-power ultrasonic irradiation at certain sound amplitudes.[16]

Herein we report the simple synthesis of homogeneous aragonite crystals with structural complexity by applying the standard vapor diffusion method to particles of a hydrophilic block copolymer.[17] These particles are composed of a triblock copolymer, poly(diethylaminoethyl methacrylate)-*b*-poly(*N*-isopropylacrylamide)-*b*-poly(methacrylic acid) (PDEAEMA-*b*-PNIPAM-*b*-PMAA), in which the poly(methacrylic acid) core is cross-linked by 1,3-diisopropylenebenzene.[18,19] The current process, contrary to previously reported syntheses, does not rely on an excess of inorganic metal ions nor the presence of a whole assembly of macromolecules or surfactants; only cheap and commonly accessible chemicals are required for the polymer preparation as well as a small amount of polymer template particles under bio-inspired crystallization conditions, that is, water at ambient pressure and temperature. Furthermore, the experiment is particularly easy to set up.

The beneficial and useful application of block copolymers with more than one hydrophilic block in crystallization has been known for several years.[20,21] So-called "double hydrophilic block copolymers" are currently used to mimic the processes occurring in natural biological materials. They consist of two hydrophilic blocks: one is a polyelectrolyte, and thus strongly interacts with crystal surfaces, and the other one is a non-ionic block, which provides the water solubility without interacting with the crystal.

The current system is such that it contains both an outer positive and an inner negative polymer block, the poly(diethylaminoethyl methacrylate) and poly(methacrylic acid) PDEAEMA and PMAA blocks, respectively, which can interact with both ions and different crystal moieties and faces. In this way, its role is expected to act as an ion sponge and to nucleate and stabilize nanocrystals which will constitute the building units of a crystalline superstructure. The PNIPAM part is expected to mediate sufficient steric stability to the particles throughout all steps of the process at room temperature where PNIPAM is hydrophilic. PDEAEMA-PNIPAM-*b*-PtBMA/MAA (cross-linked) also exhibits some hydrophilic microgel properties, which are provided mostly by the third block (PMAA). The hydrodynamic diameter of the microgel particles dispersed in water is about 1 μm, but after drying, TEM images show an average particle size of about 200 nm with a narrow size distribution between 170 and 220 nm.[19] Thus, the size of these spherical microgels can vary by swelling according to the medium (dried or in water) in which they are placed.

Precipitation experiments were performed using the so-called vapor diffusion method, with calcium carbonate synthesized by the diffusion of carbon dioxide vapor (obtained from the thermal decomposition of ammonium carbonate) into a calcium chloride solution (0.01 M) mixed with very small amounts of PDEAEMA-PNIPAM-*b*-PtMA/MAA (10^{-4} mg mL^{-1}, 0.1 ppm). It is emphasized that the relative ratio of these compounds is so high that the polymer practically does not contribute by weight to the final crystals (ratio $CaCO_3$/block copolymer $\leq 10^4$:1), that is, it is essentially its influence on nucleation which is relevant.

Scanning electron microscopy (SEM) studies of a sample collected after 12 days from the bottom of the reaction flasks shows "sheaf bundle" crystals[10–12] as the predominant morphology, slightly contaminated with a few calcite rhombohedra from the free growth of $CaCO_3$ (Figure 1a). A higher magnification (Figure 1b) reveals the high uniformity of this superstructure morphology and the quite narrow size distribution with a diameter of about 60 μm. It will be shown below that all the superstructures have been heterogeneously nucleated at interfaces. We therefore assume that the calcite contamination arises from the co-occurrence of free calcite nucleation in homogeneous solution, which cannot be completely suppressed by the very low concentrations of polymer modifier employed (0.1 ppm).

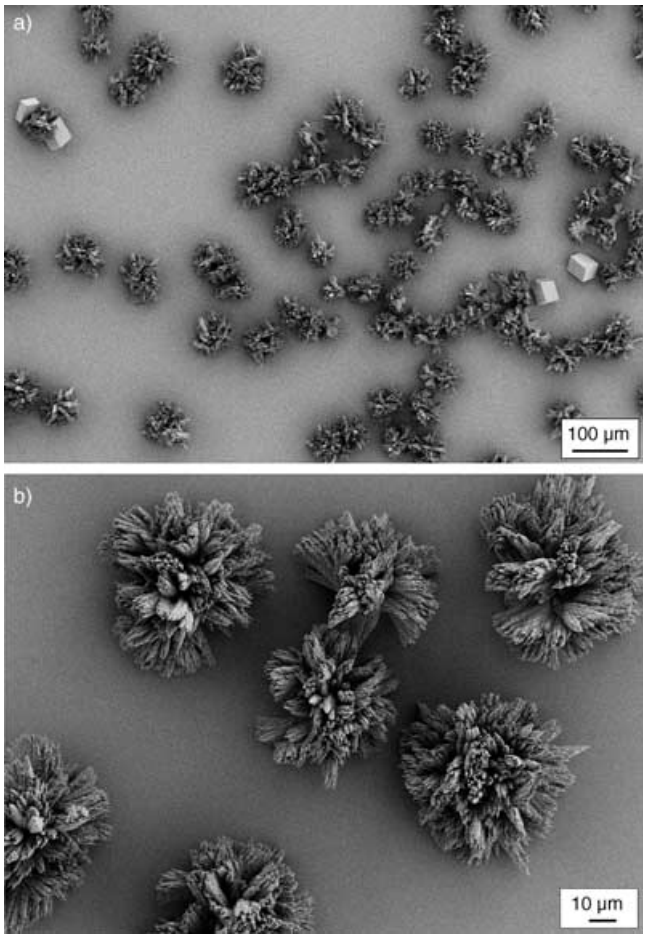

Figure 1. Lower (a) and higher (b) magnification SEM images showing a rather narrow distribution of "sheaf bundle" crystals at the bottom of the precipitation flask.

The identification of the phase of the synthesized $CaCO_3$ was carried out by X-ray powder diffraction (XRD) analysis. The XRD pattern of the sample displays the following diffraction peaks (2θ [°]): 26.12, 27.10, 32.74, 33.06, 36.12, 37.29, 37.89, 38.48, 39.42, 41.27, 43.01, 45.96, 48.44, 50.25, 52.44, and 52.92, which can be correlated to the (hkl) indices (111), (021), (121), (012), (200), (031), (112), (130), (211), (220), (221), (202), (132), (113), (321), respectively, of pure aragonite. For the sample collected from the bottom of the flask, peaks of rhombohedral calcite are also observed (diffraction peaks 2θ [°] (hkl): 29.27 (104), 39.42 (202), 47.36 (018)). These results are in agreement with the SEM observations. The identification of the phase of these crystals was also confirmed by Fourier transform infrared (FTIR) spectroscopy, which showed characteristic vibrational bands at 699, 711, 852, and 1082 cm^{-1}. The characteristic vibrational band corresponding to the asymmetric C–O stretch is 1469 cm^{-1} for aragonite and 1422 cm^{-1} for calcite. However, the broadness in this wavenumber region means that it is not possible to assign the band at 1445 cm^{-1}.

Nucleation at interfaces is also proven by analyzing finer details of the "sheaf bundles". Analysis of the trunk attachment on the glass surface (Figure 2a) and the fine structure of fallen-off crystal trunks (Figure 2b) leads us to suggest that nucleation of these crystals indeed occurs from the two-dimensional structure already present at the flat end of the trunk. The central hole in the trunk even has the correct size (of about 1 μm) to formerly have hosted one of the microgel particles of the polymer, that is, one polymer particle promotes the heterogeneous nucleation of one crystal superstructure. This view is supported by attachment of the externally positively charged particles (outer PDEAEMA layer) to the negatively charged glass surface at the starting pH value of 5.8 for crystallization, as shown by the adsorption of positive dyes or positively charged latexes onto the glass slide (see also the Supporting Information for the adsorption of the triblock copolymer particle).

Other experiments were performed to understand how such stable aragonite crystallization can occur under ambient conditions. Figure 3 presents TEM measurements performed

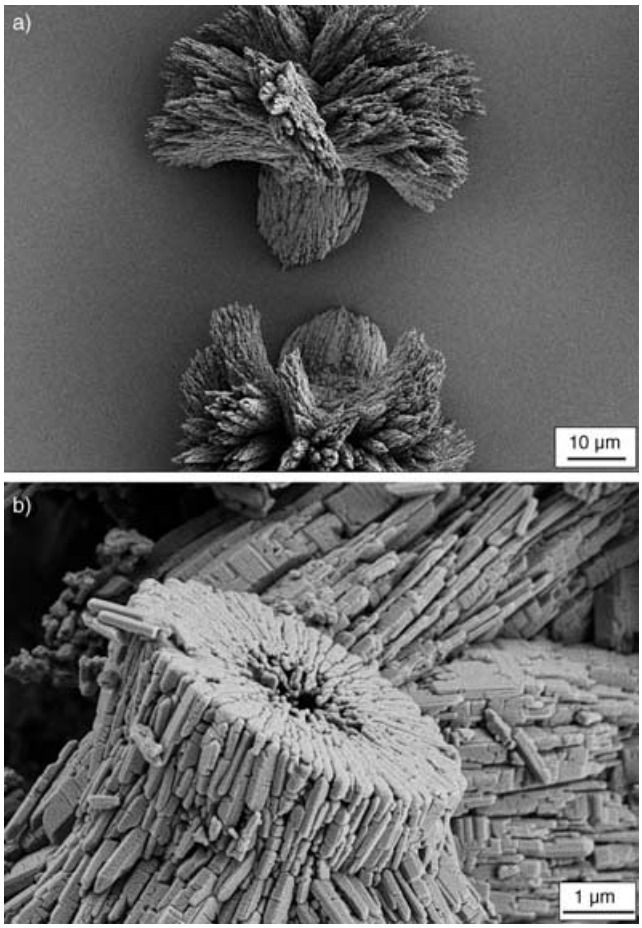

Figure 2. SEM images showing the trunk attachment to the glass wall (a) and the root (b) of a fallen-off "sheaf bundle" crystal.

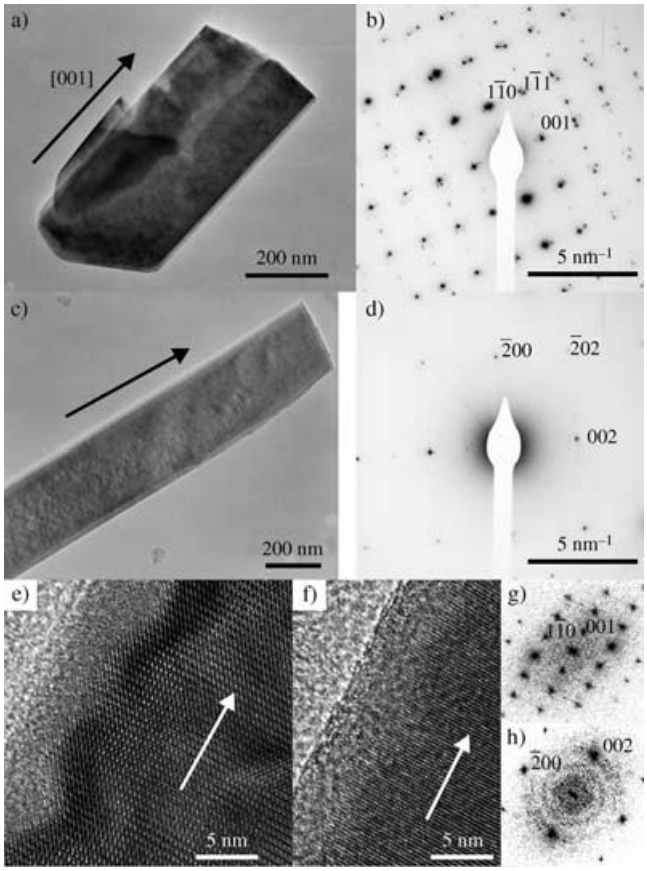

Figure 3. TEM overview images of two building blocks (a, c) and their respective electron diffractions (b, d). HRTEM image of parts of different building blocks (e, f) and their respective power spectra (g, h). The arrows indicate the [001] direction.

on the primary building blocks seen clearly in Figure 2b. These subunits are quite homogeneous and have a rodlike shape with lengths ranging from 500 nm to a few micrometers (Figure 3a and 3c). Their diffraction patterns are in some cases typical of mesocrystals such as the particle presented in Figure 3a (Figure 3b; in this case the crystal is oriented along the [110] direction) or typical of a single crystal such as the one presented in Figure 3d which is characteristic of the [010] zone axis. In both cases the long axis of the crystal is [001].

High-resolution TEM (HRTEM) was used to study the crystallinity and the surface of the particles (Figure 3e and f). The particles show a well-defined crystalline core as demonstrated by their power spectra (PS, Figure 3g and 3h), which are characteristic of single crystals viewed along the [110] and [010] directions, respectively. Surprisingly, they also show a clearly developed amorphous layer of around 5-nm thickness on their surface. This layer can not be formed by organic compounds such as the 1-μm polymer template used to induce the nucleation, and in fact this thin layer starts to crystallize slowly under the intense electron beam of the microscope. This observation suggests that this layer is composed of amorphous calcium carbonate (ACC), as was found recently on the aragonite platelets of nacre.[22] Thus, the above observations show the possibility to retrosynthesize the amorphous-layer-coated aragonite platelets in nacre by using the current synthetic polymers and crystallization conditions. The exact reason for the stabilization of the aragonite polymorph by a protective ACC layer is as yet unknown and the subject of ongoing work. Nevertheless, this amorphous "coating" could protect the aragonite against recrystallization when in contact for longer times with water.

Finally, experiments were also performed with higher polymer concentrations (10^{-3} to 1 mg mL^{-1}), while keeping the $CaCl_2$ concentration (0.01 M) constant. The increase leads first to a higher heterogeneity of the crystals until the specific crystal shape disappears. Only the mineralization of the microgel particles towards amorphous composite structures could be observed at the highest polymer concentrations (Figure 4), because of the lower available mineral concentration for each polymer particle. Dynamic light scattering (DLS) investigations confirmed the interactions between the core of the particle, which is mainly composed of acidic groups (PMAA), and the calcium ions of the solution. Indeed, DLS studies have shown that an increase in the ionic strength of the solution leads to a decrease in the average particle diameter of the stabilizing microgel particles (the average diameter of the triblock particles is ca. 1000 nm in water[19] whereas it decreases to ca. 800 nm in 0.01 M $CaCl_2$ solution). The increase in the pH value in the experimentally important range from the starting value of 5.8 to the end value of 9.5 slightly increases the size of the particles to 1200 nm as a consequence of PMAA charge repulsion in the core.

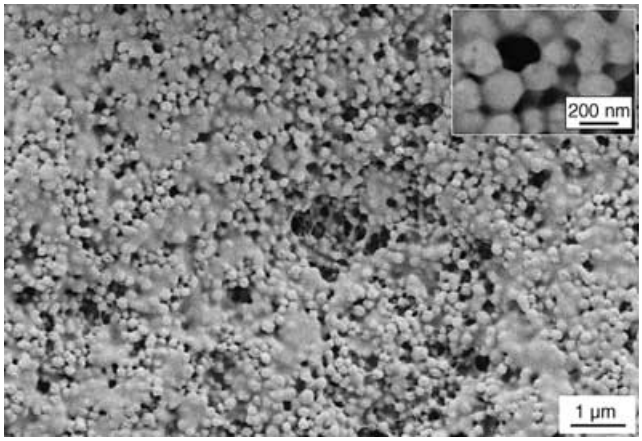

Figure 4. SEM images at lower and higher (inset) magnification of the mineralized polymer microgels (1 mg mL^{-1}).

Presumably the higher polymer concentrations model the very early stages of the formation of the "sheaf bundles". The amphoteric microgels are strong enough to bind all counterions and amorphous intermediates up to a critical concentration. When the binding concentration is exhausted (which is the case for concentration/weight ratios of $CaCl_2$/polymer greater than 1:1), this highly concentrated salt phase can specifically nucleate the aragonite phase, presumably as a result of the stabilization effects specific for the precursor-loaded polymer. The hydrogen exchange between the amine and the acid blocks could be expected to contribute to this effect. Indeed, such an interaction has been observed in the diblock copolymer poly(diethylaminoethyl methacrylate)-*b*-poly(methacrylic acid) and led to insolubility in water even at high pH values.[23] However, in the case of the triblock microgel particles here, their solubility and their size in water (ca. 1000 nm) prove that the interaction between the outer poly(diethylaminoethyl methacrylate) block and the inner poly(methacrylic acid) block is only of minor importance. Apparently, both the reduced mobility of the poly(methacrylic acid) acid groups, because of cross-linking, and a shielding action of the poly(*N*-isopropylacrylamide) middle block efficiently prevent this interaction. On the basis of Figure 4 it can be suggested that the amphoteric polymer microgel increases the salt concentration in its interior/proximity as a consequence of some zwitterionic moieties (this proposal is supported by the decrease in the particle size upon the addition of salt, as evident from DLS studies), whereas the excess of the outer PDEAEMA block nucleates a ring of radially aligned primary aragonite nanocrystals (see Supporting Information). Other molecules containing tertiary amine functions also induced aragonite formation.[24] This observation is in line with a recent finding that many molluscan shell proteins found in nacre could be less acidic than previously thought.[25] However, the controlled crystallization experiment with the PDEAEMA homopolymer additive indicated the beginning of the formation of elongated aragonite particles as well as the typical calcite rhombohedra found in the experiment with polymer concentrations greater than 1 mg mL^{-1}. At lower concentrations, the morphology of the formed calcite was still modified and resulted in roughly spherical particle superstructures up to polymer concentrations of 0.01 mg mL^{-1}, when the default calcite rhombohedra are almost exclusively obtained. This observation indicates that a high local polycation concentration should be present for the aragonite nucleation (see Supporting Information). Regardless, this ring of nanocrystals, once nucleated, propagates by growth to a distance of about 20 μm from the glass wall until the single components lose vectorial alignment and fold up to the head of the aragonite superstructure.

The lower the polymer concentration, the fewer the nucleation sites, so that the most developed and diversified structures are indeed formed at the extremely low concentration of 0.1 mg L^{-1} (0.1 ppm), a reactant concentration well

below usual values chosen to modify a physicochemical process. The fact that the aragonite superstructures nucleate on the glass walls indicates that the amphoteric microgels with a cationic outer layer indeed interact with the negatively charged glass wall. This interaction was confirmed by SEM investigations (see Supporting Information). Indeed, the triblock particles were still found to be attached to the glass surface after immersion of the glass slide in the 0.01M $CaCl_2$ solution and extensive washing.

In conclusion, it has been shown that it is possible to generate aragonite crystals by the gas-diffusion technique under ambient pressure and temperature. As the employed amphoteric polymer microgels only act as a highly selective nucleation and polymorph control agent, and are already active at the lowest concentrations (0.1 mg L^{-1}, 0.1 ppm), the resulting aragonite particles are practically free from organic contaminants and can potentially be used as they are.

Furthermore, all the structures are found to adopt a structurally well-defined, highly reproducible, "sheaf bundle" morphology. This shows that propagation of a structurally confined nucleation on the micrometer scale (a ring of radially aligned aragonite nanocrystals) can lead to control of crystals with high structural complexity, even without the action of geometric confinements, templates, and outer force fields. The formed superstructures are stable against recrystallization for at least two weeks even in contact with water, thus indicating the stability of the formed aragonite in this special morphology, which is in contrast to literature reports on aragonite stability in water.[6,7] This stability could arise from the observed outer ACC layer (Figure 3) preventing the aragonite–water contact. The unexpected stability of the ACC layer in water is the subject of ongoing investigations. However, this ACC layer does not seem to perfectly protect the aragonite crystals as deduced from the observation that a single microgel particle is able to nucleate a whole trunk of apparently unconnected aragonite crystals (Figure 2). As calcite is observed as the default solution-nucleated product (Figure 1a) and there is no additional polymer available beside the microgel templates, the exclusive formation of aragonite in the complex superstructures (Figure 2) could not be explained unless a crystallographic bridge is present between the individual particles. Such a bridge extending throughout the ACC layer could then act as a nucleation site for the formation of another aragonite particle by mesoscopic transformation of ACC precursors.[26] This result means that the whole particle superstructure is crystallographically connected, thus giving a possible explanation for the finding in biomineralization that very minute amounts of additive can influence a much larger amount of inorganic crystals. The present synthetic block copolymer microgels are indeed able to selectively nucleate aragonite at 0.1 ppm at ambient conditions in water. In summary, our study reveals three important and novel points: an easy biomimetic set-up to obtain aragonite with only a negligible concentration of polymer, the presence of an ACC layer never observed before around each single crystal block of the bundle, and the probable influence of the tertiary amine in this example as opposed to acidic molecules which are normally discussed as effective crystallization additives.

Experimental Section

$CaCO_3$ synthesis: Calcium carbonate polycrystals were grown by diffusion of carbon dioxide into calcium chloride solutions according to the gas diffusion method by thermal decomposition of ammonium carbonate. Experiments were performed at room temperature (22 ± 1 °C). Two flasks containing 0.01M calcium chloride solutions (20 mL) mixed with different concentrations of DHBC particles (10^{-4}, 10^{-3}, 10^{-2}, 0.1, and 1 mg mL^{-1}) and fresh ammonium carbonate (2 g) were placed into a closed chamber (1000 cm^3). The aqueous solutions of $CaCl_2$ were prepared in doubly distilled water and bubbled with N_2 overnight before use. The decomposition of ammonium carbonate produced ammonia and carbon dioxide diffusing through 5 needle-holes pierced into the parafilm cover of the flasks. The initial solution was slightly acidic (pH 5.8) but the pH value rose to 9.5 because of the dissolved NH_3. After completion of mineral deposition (12 days), the sample was removed from solution, rinsed with filtered water and ethanol, then air-dried.

Polymer synthesis: After preparation by aqueous heterophase polymerization, cleaning by ultrafiltration, and isolating by freeze drying, the solid could easily be dispersed into water.[19]

Crystal characterizations: The crystals were washed with distilled water then ethanol and dried in air for further characterization. Powder X-ray diffraction (XRD) patterns were recorded on a PDS 120 diffractometer (Nonius GmbH, Solingen) with $Cu_{K\alpha}$ radiation. The SEM measurements were performed on a LEO 1550–GEMINI with gold-coated samples. FT-IR spectra were recorded either on a Nicolet Impact 400 or a BioRad FTS6000 spectrometer. For TEM studies one or more drops of the solution of the nanoparticles dispersed in ethanol were deposited on an amorphous carbon film. A Phillips CM200 FEG microscope, 200 kV, equipped with a field emission gun was used. The coefficient of spherical aberration was $C_s = 1.35$ nm. The average particle diameter was determined by dynamic light scattering methods with a NICOMP particle sizer (model 370, NICOMP particle sizing systems, Santa Barbara, California, USA) as well as with a commercial goniometer with a digital correlator (both ALV, Langen, Germany) and a helium–neon laser (Polytec, Waldbronn, Germany) with wavelength $\lambda =$ 633 nm. The data evaluation of the correlation functions was based on the computer program CONTIN (Provencher, 1982), which performs an inverse Laplace transformation.

Received: January 10, 2005
Revised: June 24, 2005
Published online: August 17, 2005

Keywords: block copolymers · calcium carbonate · microgels · nucleation · polymorphism

[1] Reviews in Mineralogy: *Carbonates: Mineralogy and Chemistry, Vol. 11* (Ed.: R. J. Reeder), Mineralogical Society of America, Washington, DC, **1983**.
[2] H. Cölfen, M. Antonietti, *Langmuir* **1998**, *14*, 582.
[3] Y. Kitano, *Bull. Chem. Soc. Jpn.* **1962**, *35*, 1973.
[4] K. M. Wilbur, A. M. Bernhardt, *Biol. Bull.* **1984**, *166*, 251.
[5] H. Nakahara, *Calcification of Gastropod Nacre Biomineralization and Biological Metal Accumulation* (Ed.: P. Westbroeck, E. W. De Jong), D. Reidel Publishing, Dordrecht, **1983**, pp. 225–230.
[6] A. Richter, D. Petzold, H. Hofmann, B. Ullrich, *Chem. Tech.* **1996**, *48*, 271.
[7] G. T. Zhou, Y. F. Zheng, *Neues Jahrb. Mineral. Abh.* **2001**, *176*, 323.
[8] G. Falini, S. Albeck, S. Weiner, L. Addadi, *Science* **1996**, *271*, 67.
[9] A. M. Belcher, X. H. Wu, R. J. Christensen, P. K. Hansma, G. D. Stucky, D. E. Morse, *Nature* **1996**, *381*, 56.

[10] A. L. Litvin, S. Valiyaveettil, D. L. Kaplan, S. Mann, *Adv. Mater.* **1997**, *9*, 124.
[11] B. R. Heywood, S. Mann, *Chem. Mater.* **1994**, *6*, 311.
[12] D. Rautaray, A. Banpurkar, S. R. Sainkar, A. V. Limaye, N. R. Pavaskar, S. B. Ogale, M. Sastry, *Adv. Mater.* **2003**, *15*, 1273.
[13] H. K. Park, I. Lee, K. Kim, *Chem. Commun.* **2004**, *1*, 24.
[14] L. Mei, B. Lebeau, S. Mann, *Adv. Mater.* **2003**, *15*, 2032.
[15] J. Küther, G. Nelles, R. Seshadri, M. Schaub, H.-J. Butt, W. Tremel, *Chem. Eur. J.* **1998**, *4*, 1834.
[16] G.-T. Zhou, J. C. Yu, X.-C. Wang, L.-Z. Zhang, *New J. Chem.* **2004**, *28*, 1027.
[17] L. Addadi, J. Moradian, E. Shay, N. G. Maroudas, S. Weiner, *Proc. Natl. Acad. Sci. USA* **1987**, *84*, 2732.
[18] K. Tauer, V. Khrenov, *Macromol. Symp.* **2002**, *179*, 27.
[19] K. Tauer, V. Khrenov, N. Shirshova, N. Nassif, *Macromol. Symp.* **2005**, in press.
[20] H. Cölfen, *Macromol. Rapid Commun.* **2001**, *22*, 219.
[21] S. H. Yu, H. Cölfen, *J. Mater. Chem.* **2004**, *14*, 2124.
[22] N. Nassif, N. Pinna, N. Gehrke, M. Antonietti, C. Jäger, H. Cölfen, **2005**, *Proc. Natl. Acad. Sci. USA*, submitted.
[23] K. Tauer, M. Mukhamedjanova, unpublished results.
[24] N. Nassif, J. Polleux, unpublished results.
[25] F. Marin, G. Luquet, *C. R. Palevol* **2004**, *3*, 469.
[26] H. Cölfen, S. Mann, *Angew. Chem.* **2003**, *115*, 2452; *Angew. Chem. Int. Ed.* **2003**, *42*, 2350.

